Published online 11 December 2013 Nucleic Acids Research, 2014, Vol. 42, No. 5 2945–2957
doi:10.1093/nar/gkt1289

Evidence for G-quadruplex in the promoter of *vegfr-2* and its targeting to inhibit tumor angiogenesis

Erica Salvati[1,†], Pasquale Zizza[1,†], Angela Rizzo[1], Sara Iachettini[1], Chiara Cingolani[1], Carmen D'Angelo[1], Manuela Porru[1], Antonio Randazzo[2], Bruno Pagano[2], Ettore Novellino[2], Maria Elena Pisanu[3], Antonella Stoppacciaro[3], Francesca Spinella[4], Anna Bagnato[4], Eric Gilson[5,6], Carlo Leonetti[1] and Annamaria Biroccio[1,*]

[1]Experimental Chemotherapy Laboratory, Regina Elena National Cancer Institute, Rome, Italy, [2]Laboratory of Molecular Pathology, Department of Pharmacy, University of Naples ''Federico II'', Naples, Italy, [3]Department of Clinical and Molecular Medicine, University of Rome ''La Sapienza'', Rome, Italy, [4]Laboratory of Molecular Pathology, Regina Elena National Cancer Institute, Rome, Italy, [5]Institute for Research on Cancer and Aging, Nice (IRCAN), Nice University, CNRS UMR7284/INSERM U1081, Faculty of Medicine, Nice, France and [6]Department of Medical Genetics, Archet 2 Hospital, CHU of Nice, France

Received August 27, 2013; Revised November 16, 2013; Accepted November 18, 2013

ABSTRACT

Tumor angiogenesis is mainly mediated by vascular endothelial growth factor (VEGF), a pro-angiogenic factor produced by cancer cells and active on the endothelium through the VEGF receptor 2 (VEGFR-2). Here we identify a G-rich sequence within the proximal promoter region of *vegfr-2*, able to form an antiparallel G-quadruplex (G4) structure. This G4 structure can be efficiently stabilized by small molecules with the consequent inhibition of *vegfr-2* expression. Functionally, the G4-mediated reduction of VEGFR-2 protein causes a switching off of signaling components that, converging on actin cytoskeleton, regulate the cellular events leading to endothelial cell proliferation, migration and differentiation. As a result of endothelial cell function impairment, angiogenic process is strongly inhibited by G4 ligands both *in vitro* and *in vivo*. Interestingly, the G4-mediated antiangiogenic effect seems to recapitulate that observed by using a specific interference RNA against *vegfr-2*, and it is strongly antagonized by overexpressing the *vegfr-2* gene. In conclusion, we describe the evidence for the existence of G4 in the promoter of *vegfr-2*, whose expression and function can be markedly inhibited by G4 ligands, thereby revealing a new, and so far undescribed, way to block VEGFR-2 as target for anticancer therapy.

INTRODUCTION

Angiogenesis, the process by which the existing vascular network expands to form new blood vessels, plays an important role in a number of physiological and pathological processes, including tumor growth (1). Tumor angiogenesis is considered a pivotal process for cancer progression, as the tumor cells have an absolute requirement for new blood vessels to nourish their growth and to facilitate metastasis (2,3). The formation of new blood vessels is tightly regulated by a balance in pro- and antiangiogenic factors. During tumor growth, the balance is shifted and favors pro-angiogenic factors, a process referred as angiogenic switch (4). Following the adaptation of an angiogenic phenotype, tumor produces and secretes pro-angiogenic molecules, which activate the endothelial cells (EC) of nearby blood vessels, such as vascular endothelial growth factor (VEGF) (5–7), basic fibroblast growth factor (8), epidermal growth factor (9), platelet-derived growth factor (PDGF) (10) and angiopoietins (11,12). Among these, VEGF-A—the prototype member of VEGF family—is arguably the most important factor implicated in tumor angiogenesis (13). VEGF-A signals via the binding to high-affinity tyrosine kinase receptors expressed on the surface of EC such as VEGF receptor 1 (VEGFR-1;

*To whom correspondence should be addressed. Tel: +39 06 52662569; Fax: +39 06 52662592; Email: biroccio@ifo.it

†These authors contributed equally to the paper as first authors.

also called flt-1) and VEGF receptor 2 (VEGFR-2; also called kinase insert domain receptor (KDR) in human or flk-1 in mouse), the receptor functionally more relevant in the transduction of pro-angiogenic stimuli incoming from tumor cells (14–16). Binding of VEGF-A to VEGFR-2 results in autophosphorylation of the receptor, and the phosphorylated tyrosine residues activate signaling cascades, including the Ras and Rho GTPase family members, eventually leading to cellular processes involved in angiogenesis (17), such as vesicle trafficking, cytoskeleton regulation, cell polarity, microtubule dynamics and membrane transport (18). Discovery of VEGF/VEGFR-2 signaling in controlling tumor angiogenesis prompted the development of a number of drugs targeting the VEGF pathway as part of anticancer therapy. Among these drugs are antibodies against VEGF-A or its receptors, engineered proteins that mimic VEGF receptors and small molecules inhibitors that preferentially target VEGFR-2. However, although striking benefits of anti-VEGF/VEGFR therapy are observed in preclinical models, the outcomes of clinical trials have been less impressive (19).

G-quadruplex (G4) ligands are small molecules able to bind and stabilize G4 structures widely described at the telomeric ends of chromosomes (20,21). As a result of research on telomeric G4 and the cellular consequence of targeting them with small molecules that stabilize these structures, their biological and therapeutic significance is well appreciated and continues to be an active field of drug discovery (22). Interest in the more general therapeutic significance of G4 has expanded during the past decade to include G4 structures in the promoters of a wide range of genes important in cell signaling, recognized as hallmarks of cancer: c-Myc, c-Kit and K-Ras (self-sufficiency), pRb (insensitivity), Bcl-2 (evasion of apoptosis), VEGF-A (angiogenesis), hTERT (limitless replication) and PDGF-A (metastasis) (23). Many G4 in gene promoters have physicochemical properties and structural characteristics that make them druggable, and their structural diversity suggests that a high degree of selectivity might be possible. More interestingly, G4 DNA structures have been now visualized in human cells, corroborating the application of stabilizing ligands as a new class of anticancer agents (24,25). In this context, a first-in-class G4-interactive compound, quarfloxin, progressed to Phase II clinical trials for cancer, providing proof of principle for the potential therapeutic viability of targeting these structures.

In this article, we provide evidence for the existence of G4 in the promoter of VEGFR-2, highlighting a new gene for which the presence of G4 could have particular therapeutic potential. The functional relevance of this observation has been directly achieved by using G4 ligands, corroborating the application of stabilizing ligands in a cellular context to target G4 and intervene with their function.

MATERIALS AND METHODS

Cell culture, treatment and transfection/infection

Human umbilical vascular endothelial cells (HUVEC) were purchased from Lonza (Group Ltd, Basel, Switzerland) and maintained in EBM-2 medium supplemented with growth factors (Lonza). Human cervical (Hela) and breast (CG5) cancer cell lines were maintained in Dulbecco's Modified Eagle's Medium (D-MEM) supplemented with 10% Foetal Calf Serum (FCS) (26). The green fluorescent protein (GFP), RhoA(L63) and Rac1(L61) recombinant adenoviruses (Cell Biolabs Inc., San Diego, CA, USA) were used at multiplicity of infection (MOI) 1000. For DNA and small interfering RNA trasfection, HUVEC were transfected with lipofectamine (Invitrogen SRL, Milan, Italy) with CMV-Hygro (empty) and pCMV-HygroVEGFR-2 plasmids (Sino Biological, Beijing, P.R. China). For VEGFR-2 small interfering RNA, the ON-TARGET plus Smart pool KDR (Dharmacon, Thermo Fischer Inc., MA, USA) was used.

In situ mutagenesis

The pGL3-VEGFR2-780 luciferase reporter plasmid (Addgene plasmid 2130727) (27) was mutagenized by using the Quick Change Site directed Mutagenesis kit (Agilent Technologies, CA, USA) with the following primers: FW: 5′-TGA GGG GCG GAG CTG GCC GCA CGG GAG A-3′; RW: 5′-TCT CCC GTG CGG CCA GCT CCG CCC CTC A-3′.

Luciferase assay

HeLa cells transfected with the pGL4-CMV-Luc (Promega, WI, USA), wild-type (wt) or mutated pGL3-VEGFR2-780 together with the pBABEpuro plasmid and selected in puromicin were exposed to RHPS4 (3,11-difluoro-6,8,13-trimethyl-8H-quino[4,3,2-kl]acridinium methosulfate) for 72 h and then processed for β-galactosidase activity assay (Promega). Luminescence was quantified by a Wallac 1459 Micro Beta TRILUX Luminescence counter (Perkin Elmer, MA, USA).

Circular dichroism

The oligonucleotides 5′-GGG TAC CCG GGT GAG GGG CGG GG-3′ (wt) and 5′-GGG TAC CCG AGT GAG GGG CGG GG-3′ (mut) (Primm SRL, Italy) were purified by HPLC. Oligonucleotide samples were prepared in potassium phosphate buffer (70 mM KCl, 10 mM KH_2PO_4, 0.2 mM EDTA, pH 7.0) at a concentration of 15 μM. Circular dichroism (CD) spectra and CD melting curves of oligonucleotide samples were recorded by using a Jasco J-715 spectropolarimeter equipped with a Jasco JPT-423-S temperature controller. CD spectral scans were accumulated over the wavelength range 210−320 nm at 20°C. The spectra were recorded at a scan rate of 100 nm/min with a response of 1 s at 2.0-nm bandwidth and were averaged over 5 scans. Buffer baseline was subtracted from each spectrum. CD melting and annealing curves were recorded as a function of temperature in the range 20–90°C at 264 nm with a scan rate of 0.5°C/min.

DNA polymerase stop assay

DNA polymerase stop assay was performed as described (28). Briefly, a mixture of DNA template (77-mer with a Pu27 insert, 5′-CTG GAG ATC CCC GCC GGG TAC

CCG GGT GAG GGG CGG GGC TGG CCG CAC GGG AGA GCC CCC TAT AGT GAG TCG TAT TA-3′) and 5′-end-labeled 18-mer template (5′-TAA TAC GAC TCA CTA TAG-3′) was heat-denatured and reannealed in the absence or presence of KCl or G4 ligands and then processed for DNA polymerase reaction. The products were resolved on denaturing polyacrylamide gel and visualized by Phosphorimager (Bio-Rad, CA, USA).

Real-time quantitative PCR

RNA was extracted with Trizol reagent (Invitrogen) and converted to complementary DNA with the SuperScript ®VILOTMkit (Invitrogen). Real-time quantitative PCR (qPCR) was performed in triplicate using the LightCycler system (Roche Diagnostics, IN, USA). The following primers were used: (forward) 5′-TGG GGG AGC GTG TCA GAA T-3′ and (reverse) 5′-CCG CTT TAA TTG TGT GAT TGG AC-3′. The specificity of each PCR products was controlled using the melting curve. The relative gene expression levels were calculated using the 2-ΔΔCt method, where Ct represents the threshold cycle, and cyclophilin-A was used as a reference gene.

Immunofluorescence

Cells fixed with 2% paraformaldehyde were incubated with the following primary antibodies: rabbit polyclonal anti-FLAG (Sigma-Aldrich, 1:300) and mouse monoclonal anti-VEGFR2 (Fitzgerald, MA USA, 1:100). Then, samples were incubated with the secondary antibodies (goat anti-mouse FITC or goat anti-rabbit FITC; Jackson Immunoresearch, Suffolk, UK; 1:250), stained with TRITC-conjugated Phalloidin (Sigma-Aldrich, 1:5000) and nuclei were counterstained with DAPI. The glasses were analyzed with a Leica DMIRE2 microscope equipped with a Leica DFC 350FX camera and elaborated by Leica FW4000 deconvolution software (Leica, Solms, Germany).

Fluorescence Associated Cell Sorting analysis

Cell cycle analysis was assessed by staining cells with Propidium Iodide solution, whereas apoptosis was evaluated by AnnexinV staining (29). For immunofluorescence (IF) quantification, untreated and treated HUVEC were incubated with the anti-VEGFR-2 primary antibody (Fitzgerald, MA, USA), stained with FITC-conjugated goat anti-mouse antibody (Jackson Immunoresearch, Suffolk, UK) and analyzed by flow cytometry using FACScalibur (Becton-Dickins, San Jose, CA, USA).

EC functional assays

EC were pretreated with G4 ligands for 72 h to achieve VEGFR-2 downregulation, then starved for 24 h in presence or absence of G4 ligands and processed for the following functional assays:

Cell proliferation

MTT (3-(4,5-Dimethylthiazol-2-yl)-2,5-Diphenyltetrazolium Bromide) assay was performed in treated and untreated cells stimulated with 10 ng/ml VEGF-A (R&D Systems Inc. MN, USA) for 24 h. Cells were incubated with MTT solution (Sigma-Aldrich), and the purple formazan crystals were dissolved in isopropanol. Optical densities (OD) at 540 nm was determined on microplate reader.

Cell migration

Chemotaxis was performed in triplicate in a 48-microwell chemotaxis chamber using 8-μm-pore-size polycarbonate filters (NeuroProbeInc, MD, USA) coated with murine collagen type IV (Becton and Dickinson). The lower compartment of each chamber was filled with medium containing 0.1% bovine serum albumin, as negative control, or 10 ng/ml VEGF-A. Each well of the upper compartment was filled with EC containing medium. After 4 h of incubation, the chemotaxis assay was stopped, and cells on the filter were stained using crystal violet. Cells on five random fields on the lower face of the filter were counted at 40× magnification.

In vitro angiogenesis

EC differentiation into tubular structures (TS) was assessed as previously reported (30). Untreated and treated EC were seeded on Matrigel-coated wells in presence or absence or 60 ng/ml VEGF-A. The presence of TS was monitored from 4 to 16 h after plating, and images were captured by phase contrast microscopy. Quantification of TS formation was expressed by the mean number of branching points in five fields.

In vivo angiogenesis

Matrigel (Becton Dickinson) mixed with VEGF-A (100 ng/ml), Tumor Necrosis Factor α (TNFα) (2 ng/ml) (R&D Systems, Inc. MN, USA) and Eparin (Hospra, Napoli, Italy) in presence or absence of G4 ligands was injected subcutaneously in C57/BL6 mice ($n = 8$ for each group). After 4 days from Matrigel injection, plugs were removed and processed for hemoglobin quantization using Drabkin solution. The OD of each sample was determined at 540 nm (and normalized for 100 mg of Matrigel).

RhoA and Rac1 activation assay

Rac1 pull down: the sepharose-GST-PAK-CD beads, which specifically pull down the GTP-bound Rac1, were prepared by using the pGEX-PAK-CD (CRIB domain aa56–141) expression vector as described (31). At the end of treatments, cells lysed in RIPA buffer were incubated with sepharose-GST-PAK-CD for 45 min at 4°C. Beads were successively washed, resuspended in sample buffer and processed for western blotting against Rac1 (upstate). For detection of active RhoA, cell samples were processed with the RhoA G-Lisa assay kit (Cytoskeleton Inc. Denver, CO, USA). Luminescence emissions were quantified by Wallac 1459 Micro Beta TRILUX Luminescence counter (Perkin Elmer, MA, USA)

Immunohistochemistry

CG5 cells were xenografted in nude mice to induce tumor take as reported (32). Untreated and RHPS4

(15 mg/kg)-treated tumors were explanted at days 7 and 14, and immunohistochemistry analysis was performed. Five-micrometer frozen sections from three different tumors, obtained from at least three levels of the different tumor masses, were then immunostained with anti-CD34 (Pharmingene DB) or anti-VEGFR-2 (Fitzgerald, MA, US, USA) and counterstained with hematoxylin. Vessels were evaluated in 10 high-powered field (HPF) of each section of tumor and peritumoral areas where vessels were most frequent and reported as mean ± SD/HPF (40 × magnification) of the tree mice for each time point.

RESULTS

The *vegfr-2* gene contains a G4 structure in the promoter and its expression is inhibited by G4 ligands

VEGFR-2 is the main receptor expressed on the surface of EC regulating tumor angiogenesis. Here, based on computational analysis with the QGRS G4 structure prediction software (33), we identified a G-rich strand in the promoter (region from −117 to −94) of *vegfr-2* gene (Figure 1A) whose probability to form G4 structures (G-score) is similar to that of human telomeric repeats stretch (Figure 1B). To experimentally validate the predictive analysis, we investigated the structure adopted by an oligonucleotide reproducing the putative G4-forming region of *vegfr-2* promoter by CD (34–36). The CD bands of DNA samples are generated when the bases are chirally oriented with respect to each other, i.e. when the DNA is structured. Owing to the heterotypic nature of the two faces of guanines, each G-tetrad can stack onto the adjacent one through the same (head-to-head or tail-to-tail) or the opposite (head-to-tail) face, leading to a homopolar or heteropolar stacking, respectively. The former happens when two Gs in a raw in the same strand have opposite glycosidic bond angle conformation (i.e. anti-syn or syn-anti), whereas the latter happens when the two Gs possess the same glycosidic bond angle (i.e. anti-anti or syn-syn). In our case, experimental CD spectrum of the oligonucleotide in the presence of KCl is characterized by two positive bands at 263 and 285 nm, and a negative band at 237 nm, that are typical of an antiparallel G4 structure having both homopolar and heteropolar stacks (Figure 1C). Melting and annealing CD experiments showed no significant hysteresis for the oligonucleotide heating/cooling processes (Figure 1D), indicating a fast kinetics for the G4 formation and thus suggesting the formation of a unimolecular G4 structure. The capacity of the target oligonucleotide to fold into a stable G4 structure was further investigated by a Dimethyl sulfate (DMS) footprinting assay, confirming that all the guanine residues contained in that oligonucleotide resulted protected from methylation (Supplementary Figure S1A). In addition, CD melting analysis (37) was performed to verify whether a G4 ligand was able to stabilize the quadruplex structure formed by the oligonucleotide. To this aim, the pentacyclic acridine RHPS4, a small molecule originally designed to interact with G4 structures of telomeric DNA, demonstrating effectiveness in disrupting telomere maintenance mechanisms and in inhibiting telomerase activity in human tumour cells (26,38,39), was used. The results demonstrated that RHPS4 (used at a 2:1 ligand/DNA ratio), increased of about 20°C the thermal stability of the G4 (Figure 1D), thereby indicating a tight interaction with the DNA sequence of interest. Moreover, the CD spectrum was unaffected by the presence of the G4 ligand, demonstrating that the oligonucleotide/ligand interaction did not promote any conformational change in the quadruplex structure and that the G4 is maintained in the presence of the ligand (Figure 1C). Interestingly, when a point mutation was introduced in the second triplet of Gs, the CD profile changed (Supplementary Figure S1B), suggesting that the mutated sequence (mut) forms a structure different from that of 'wt' sequence (Figure 1C). The CD melting experiments performed on 'mut' show significant hysteresis in the heating and cooling processes (Supplementary Figure S1C), strongly supporting the idea that 'mut' could not adopt an intramolecular G4 structure, but because of the presence of three G clusters, it might form intermolecular structures. In addition, CD melting experiments performed in the presence of RHPS4 in solution (2:1 ligand/DNA ratio) showed that the G4 ligand was not able to stabilize the structure/structures formed by 'mut' (Supplementary Figure S1C). Consistently, the polyacrylamide gel electrophoresis assay (Supplementary Figure S1D) clearly shows that 'mut' does not exhibit a band with mobility similar to 'wt', suggesting the formation of different species having higher molecular weight. Finally, to verify if the DNA polymerase, passing toward the 5′ end of the DNA template, blocked at the guanines involved in the stabilized *vegfr-2* quadruplex, the polymerase stop assay was performed. When the DNA template containing the 'wt' G4-forming region was annealed with ^{32}P-labeled primer and incubated with Taq DNA polymerase, a potassium-dependent stop of the DNA polymerase extension was well observed at the highest salt concentrations (Figure 1E, left panel). The addition of RHPS4 to the mixture reaction, containing a lower potassium concentration, was able to stabilize the G4 structure in a dose-dependent manner, giving rise to the accumulation of stop products, which are not detectable in presence of a 'mut' oligo (Figure 1E, central and right panels).

Altogether, these data clearly demonstrate that G-rich strand located in the proximal region of *vegfr-2* promoter possesses all those chemical properties to form, under adequate conditions, G4, which, in turn, can be stabilized by a G4 ligand with the consequent block of DNA polymerase.

In light of our results demonstrating that the promoter of *vegfr-2* forms a G4 structure that can be stabilized by small molecules, we sought to determine whether this stabilization affects the transcription. When transfected into Hela cells, pGL3-wt vegfr-2-Luc drove luciferase expression into these cells and RHPS4 reduced the enzymatic activity of 'wt' vegfr-2-Luc, in a dose-dependent manner, reaching ∼70% at the highest dose (Figure 2A). The CMV-driven luciferase activity was not affected by the treatment and, more interestingly, a point mutation in the G-rich sequence of *vegfr-2* promoter was sufficient to achieve a complete rescue, strongly demonstrating that the

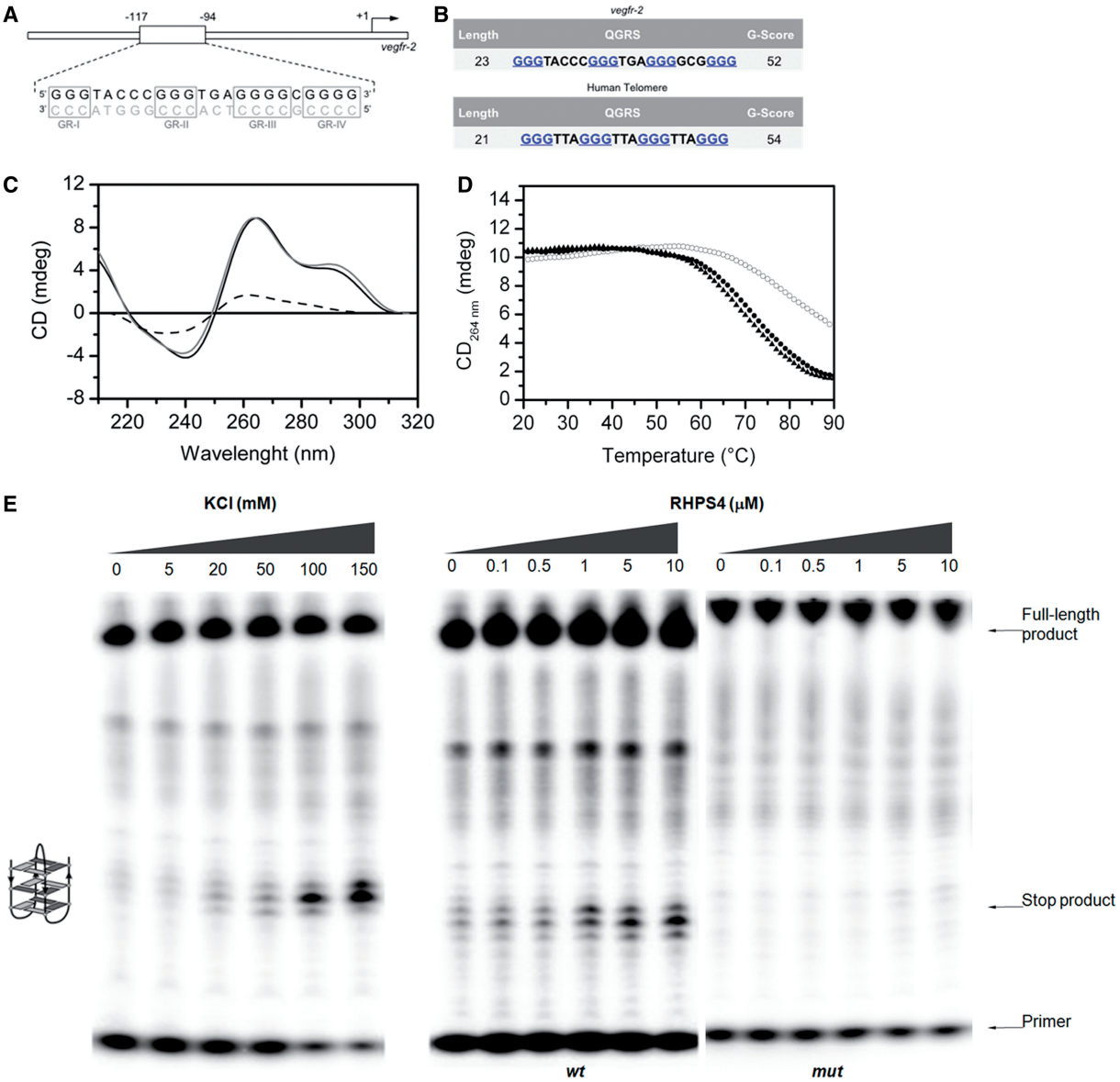

Figure 1. The vegfr-2 promoter contains a G4-forming region: (**A**) scheme of *vegfr-2* promoter G4-forming region. (**B**) Score of QGRS mapper (G4 structure prediction software, www.bioinformatics.ramapo.edu/QGRS/analyze.php) for the *vegfr-2* (from −117 to −94) promoter sequence compared with a stretch of human telomere repeats (33). (**C**) CD spectra of 5′-GGG TAC CCG GGT GAG GGG CGG GG-3′ at 20°C (black solid line), 90°C (black-dashed line) and 20°C in presence of RHPS4 (gray solid line). (**D**) CD melting (filled circles) and annealing (filled triangles) profiles of *vegfr-2* promoter sequence oligo recorded at 264 nm, and CD melting in presence of RHPS4 (empty circles). (**E**) Polymerase stop assays: the oligonucleotides underwent polymerase reaction in presence of increasing concentrations of KCl (left panel) and/or in the presence of 5 mM KCl plus increasing concentrations of RHPS4 (right panel). The accumulation of stop products indicates the presence of stabilized G4 structures impeding the DNA polymerase passage. Data shown are representative of three independent experiments with similar results.

stable G4 structure formed locally in the human *vegfr-2* promoter behaves as a transcriptional repressor *in vivo* (Figure 2A). To explore the biological consequences of these observations, we next assayed whether the expression of VEGFR-2 was affected by RHPS4 both at the transcriptional and translational levels in HUVEC. Results obtained from qPCR analysis demonstrated that intracellular levels of *vegfr-2* messenger RNA (mRNA) were reduced in a time-dependent manner starting from 24 h of treatment with the G4 ligand, reaching an inhibition of ∼90% within 72 h of drug exposure (Figure 2B). Other angiogenesis-related genes containing or not putative G4 structures in their promoter, based on bioinformatic studies, were analyzed by qPCR as possible targets of RHPS4. The results showed that some G4 targets were downregulated (vegf-A, vegfr-1, Interleukin 1 Receptor (IL1R), Chemokine Receptor 1 (CXCR-1) and Acetylcholine Receptor beta 1 (AChRβ1)), whereas others seemed to be unaffected [Fibroblasts Growht Factor Receptor (FGFR), Epidermal Growth Factor Receptors (EGFR)], consistently with the chemical diversity of the G4 structures (Supplementary Figure S2). The non-containing G4 genes (Inerleukin 10 Receptor (IL-10R) and AChRα1) remained unchanged, supporting the specificity

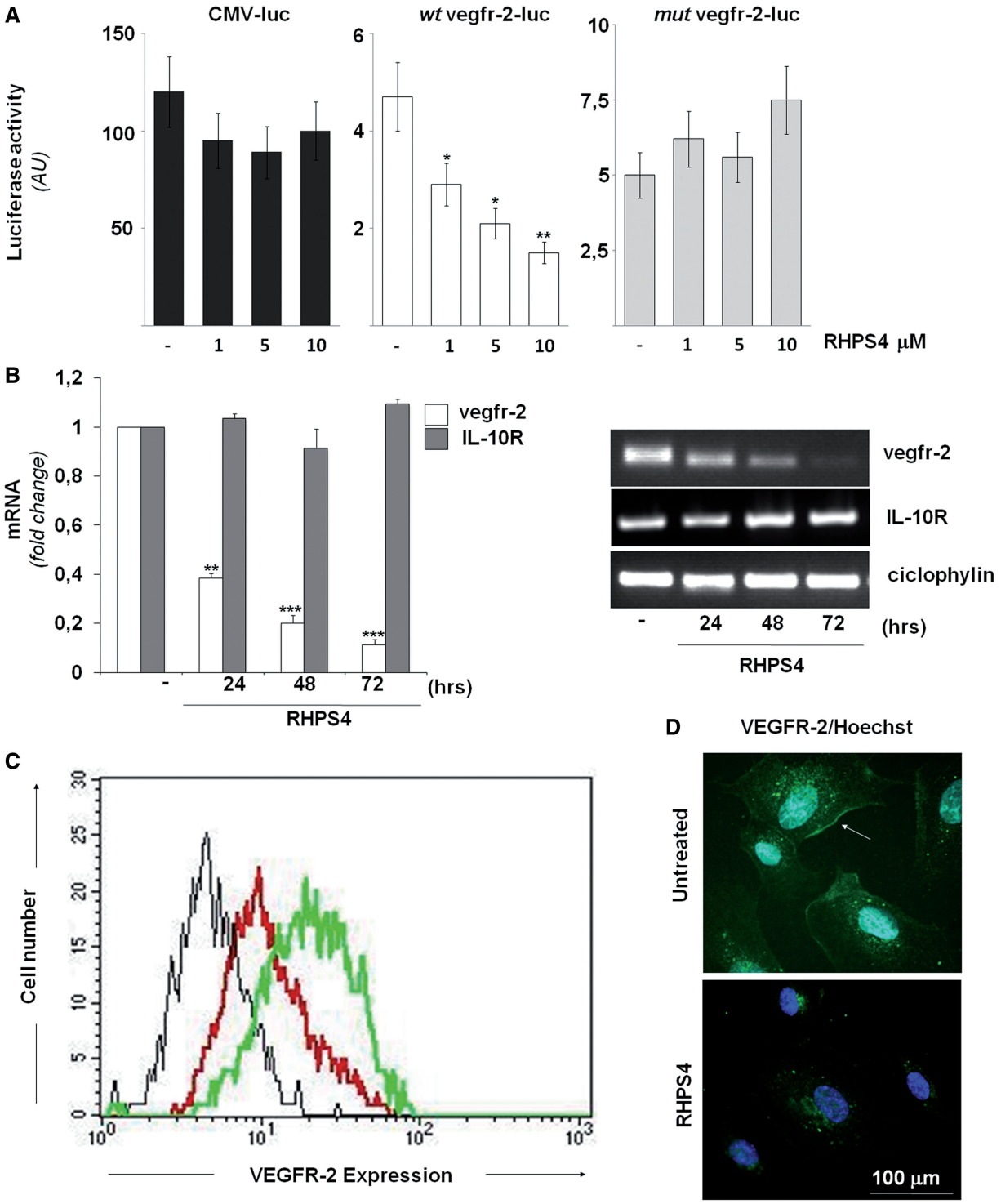

Figure 2. Stabilization of G4 inhibits VEGFR-2 expression. (**A**) HeLa cells stably expressing the indicated luciferase reporter genes were treated with the indicated concentrations of RHPS4 for 72 h and then processed for luciferase assay. Histograms represent the luciferase activity normalized on total protein content. (**B**) HUVEC cells treated with 0.5 μM of RHPS4 for the indicated times were collected, and *vegfr-2* and IL-10R mRNA expression was analyzed by qPCR. Results are expressed as fold reduction in treated versus untreated samples, after cyclofilin normalization. Picture at the bottom shows that the qPCR amplification products run on agarose gel. (**C**) HUVEC cells untreated or treated with 0.5 μM RHPS4 for 72 h were immunostained with the anti-VEGFR-2 antibody and processed for FACS analysis. Histograms represent the fluorescence intensities in the negative control (black line) untreated (green line) and treated (red line) samples. (**D**) HUVEC cells treated as described in C were analyzed for IF against VEGFR-2 and counterstained with Hoechst. Representative images at 63× magnification are shown. Arrow shows the membrane staining. Histograms in A and B show the mean values of three independent experiments, whereas panels B (lower), C and D show one representative of three independent experiments with similar results. Bars indicate means ± SD. $*P < 0.1$; $**P < 0.01$; $***P < 0.001$.

of RHPS4 (Figure 2B and Supplementary Figure S2). To verify whether inhibition of gene transcription correlated with a reduction in protein expression level, VEGFR-2 was analyzed by IF using flow cytometry, for automated quantification, and fluorescence microscopy, for morphological analysis. Fluorescence Associated Cell Sorting (FACS) analysis revealed that the treatment of HUVEC cells with RHPS4 induced ~50% reduction of cellular amount of VEGFR-2 (Figure 2C). Interestingly, the main reduction of protein was observed at the level of plasma membrane (Figure 2D), indicating that the residual VEGFR-2, detected by FACS analysis, is probably unable to respond to VEGF-A stimulation.

EC functions are inhibited by G4 ligands

The aforementioned results raise the interesting possibility that the inhibition of VEGFR-2 protein by the G4 ligand may block EC functions. Therefore, we investigated the effect of RHPS4 on VEGF-A stimulated EC proliferation, motility and differentiation—three key events in the angiogenic process (40). As expected, VEGF-A stimulated the growth of HUVEC cells (Figure 3A). Interestingly, the treatment with RHPS4 inhibited EC proliferation in a dose-dependent manner, reaching the level of unstimulated cells at 2 μM concentration. Similarly, RHPS4 almost completely abrogated VEGF-A stimulated EC migration (Figure 3B and Supplementary Figure S3A). Importantly, the exposure of HUVEC cells to RHPS4 neither affected cell viability apoptosis or senescence, nor activated DNA damage response pathway at the dose and time used (Supplementary Figure S4), strongly supporting the specific effect of the G4 ligand on the EC. Consistent with these results, when plated on Matrigel and stimulated with VEGF-A, EC aligned with one another and formed tubular structures (TS) resembling a capillary plexus (Figure 3C and Supplementary Figure S3B), whereas the addition of RHPS4 severely impaired alignment and tube formation, resulting in isolated and rounded EC, closely resembling control cells (Figure 3C and Supplementary Figure S3B). Importantly, the effects of RHPS4 on EC function appeared to be principally mediated by a reduced expression of *vegfr-2*: they recapitulated those observed by using a specific interference RNA against *vegfr-2* (Figure 3D), and they were antagonized by overexpressing the *vegfr-2* gene under the control of the CMV viral promoter (Figure 3E). The link between G4 ligand-mediated inhibition of *vegfr-2* and impairment of EC functions was reinforced by using other chemically unrelated G4 ligands, Emicoron and PPL3C, two molecules, belonging to the coronene and perilene families of ligands, respectively (41,42). Consistently with the polymerase stop assay data, PPL3C and Emicoron caused a different degree of VEGFR-2 protein reduction and impairment of EC migration (Supplementary Figure S5A–C).

Finally, the inhibitory effect of RHPS4 on the VEGF/VEGFR-2 signaling pathway was also assessed by studying RhoA and Rac1, the two major players in the regulation of actin cytoskeleton among the Rho GTP binding proteins downstream to VEGFR-2, which have been shown to be activated with a definite kinetics on VEGF-A stimulation (43). As reported in Figure 4A, unstimulated HUVEC cells showed a disorganized actin cytoskeleton in both untreated and RHPS4-treated conditions. VEGF-A induced stress fibers activation and membrane ruffles, which resulted from RhoA and Rac1 activation, respectively. Interestingly, when HUVEC cells were treated with RHPS4 before VEGF-A stimulation, the activation of both RhoA and Rac1 was completely inhibited (Figure 4A and B), strongly supporting that the G4 ligand impaired the VEGF/VEGFR-2 signaling pathway. Moreover, RHPS4-mediated inhibition of EC migration was almost completely rescued by overexpressing either the constitutively active mutant Rac1(L61) or RhoA(L63) (Supplementary Figure S6), while, in agreement with the key role of Rac1 on *in vitro* angiogenesis (44), the induction of TS in response to VEGF-A in RHPS4-treated HUVEC cells was completely recovered by overexpressing the constitutively active mutant Rac1(L61) but not RhoA(L63) (Figure 4C).

Altogether these results demonstrated that exposure of EC to a G4 ligand resulted in an impairment of EC functions and consequently of *in vitro* angiogenesis via a reduced expression of *vegfr-2*.

In vivo angiogenesis is impaired by G4 ligands

The antiangiogenic properties of the G4 ligands were further characterized *in vivo* using the Matrigel plug assay. Macroscopic analysis of Matrigel plugs containing heparin and VEGF-A injected subcutaneously in the flank of C57BL/6 mice revealed an intense vascularization that was markedly inhibited in the presence of G4 ligands (Figure 5A and Supplementary Figure S5D). The angiogenic response observed by macroscopic analysis was confirmed by the quantitative measurement of the hemoglobin content of the excised Matrigel plugs (Figure 5A and Supplementary Figure S5D). Moreover, histological examination of RHPS4-treated Matrigel plug sections showed a centripetal gradient of reduction of both invasion and peritumoral recruitment of VEGFR-2 positive cells, associated with a severe incapability to form complex vascular structures, clearly visible in the vehicle plugs (Figure 5B). Finally, the antiangiogenic activity of RHPS4 was examined in nude mice xenografted with CG5 cells. Immunohistochemical analysis of the tumor tissue sections revealed a massive decrease of both the number of vessels (CD34) and VEGFR-2 expression at the tumor stroma interface of the RHPS4-treated mice (Figure 5C and D). The impairment of VEGFR-2 expression observed by immunohistochemistry was confirmed by the quantitative mRNA measurement of the total RNA extracted from frozen tumor sections (Figure 5E).

Altogether these results clearly demonstrate that G4 ligands can have a marked effect on EC, mainly attributable to the negative modulation of VEGFR-2 expression.

DISCUSSION

G4 are four-stranded DNA structures described in gene promoter regions and are viewed as emerging therapeutic

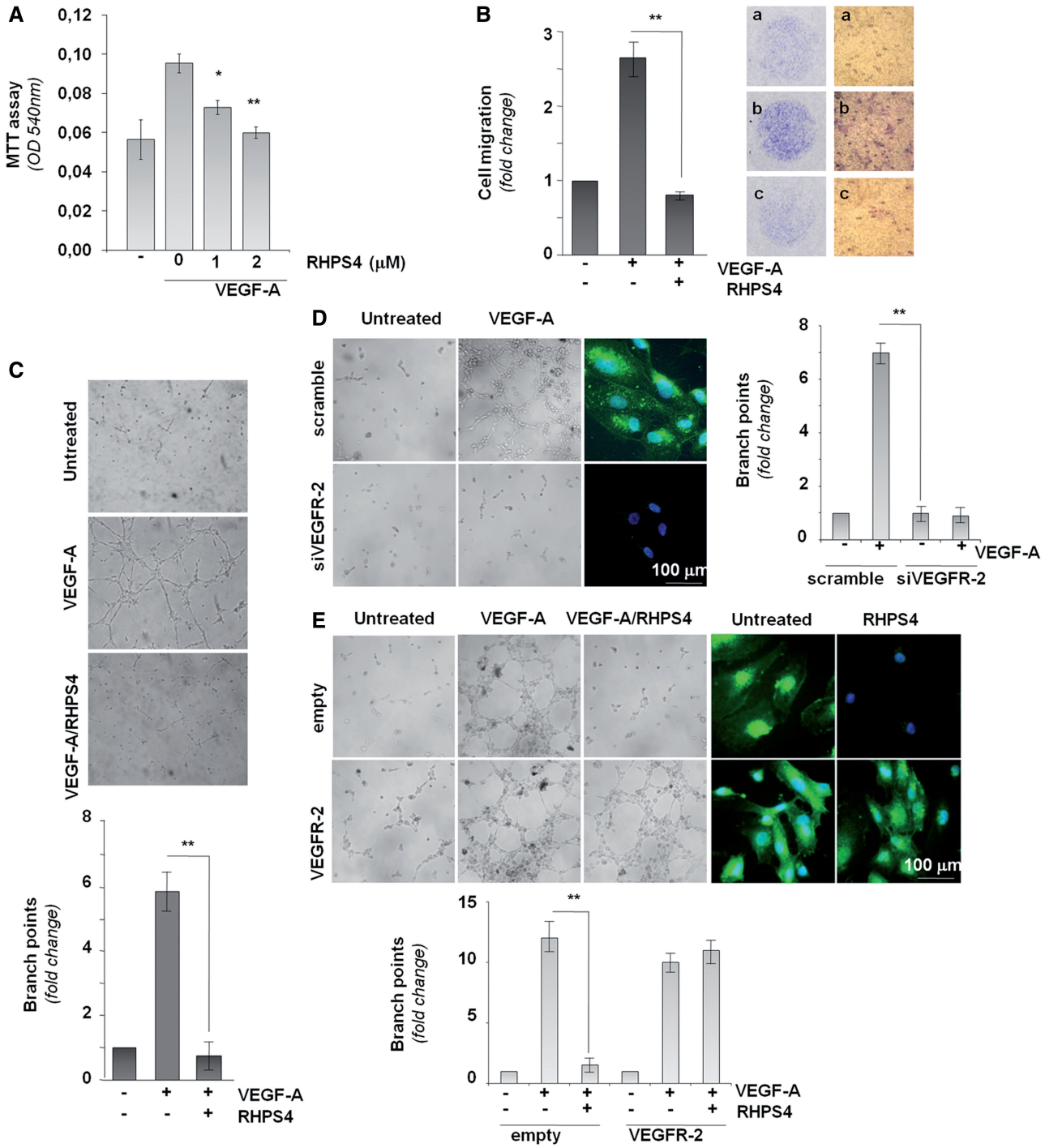

Figure 3. G4 stabilization impairs *in vitro* angiogenesis. (**A**) HUVEC cells, untreated (−) or treated with the indicated concentrations of RHPS4 for 72 h to achieve VEGFR-2 downregulation, were starved for 24 h and then stimulated with VEGF-A in presence or absence of RHPS4. Cell viability was evaluated by MTT assay. Histograms represent the absorbance values at OD 540 nm. (**B**) HUVEC cells, untreated (−) or treated with 0.5 μM RHPS4 for 72 h, were starved for 24 h in presence or absence of RHPS4 and then processed for chemotaxis assay. Histograms represent the fold change of the number of migrated cells in VEGF-A stimulated versus unstimulated condition. Pictures show migrated cells through the Boyden chamber filter (magnification: 1×, left panels, and 40×, right panels) in untreated (a), VEGF-A stimulated (b) and VEGF-A/RHPS4 treated (c) cells. (**C**) HUVEC cells treated as in B were processed for the *in vitro* angiogenesis assay. The upper panel shows representative images of TS in the indicated samples (20× magnification). Quantification of TS is reported in the lower panel. Histograms represent the mean number of branch points per field. **(D** and **E)** HUVEC cells transfected as indicated and treated as in B were processed for the *in vitro* angiogenesis assay. Representative images of TS are shown. IF pictures show VEGFR-2 staining merged with Hoechst in the indicated conditions (63× magnification). Histograms represent quantification of TS. Histograms show the mean values of three independent experiments, whereas images show one representative of three independent experiments with similar results. Bar scale = bars indicate means ± SD. $*P < 0.1$; $**P < 0.01$.

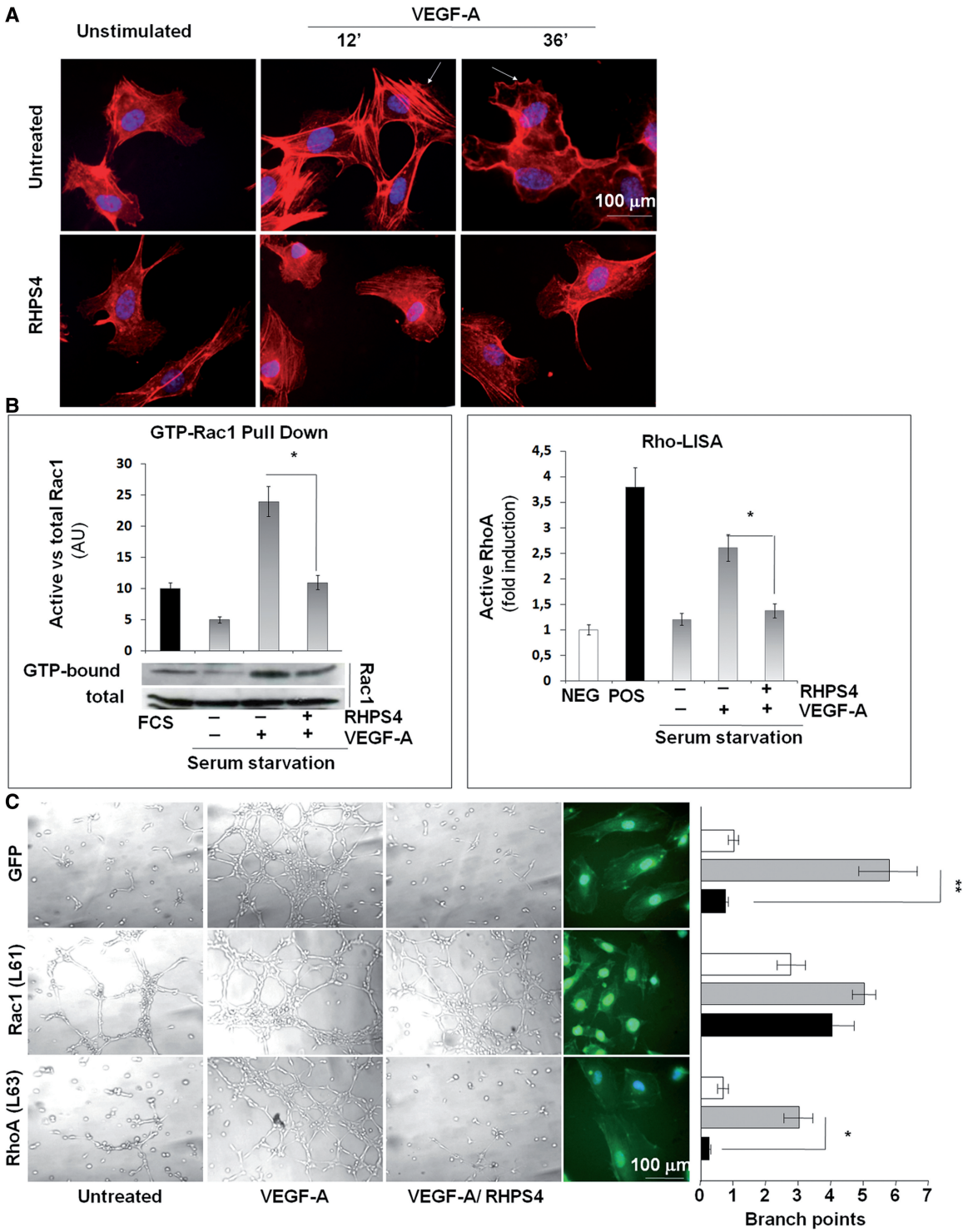

Figure 4. G4 stabilization blocks VEGFR-2 signaling. (**A**) HUVEC cells, untreated or treated with RHPS4 0.5 μM for 72 h to achieve VEGFR-2 downregulation, were starved for 24 h and then stimulated with VEGF-A for 12 or 36 min to activate RhoA and Rac1, respectively. Cells were successively fixed and stained with TRITC-conjugated Phalloidin to mark polymerized actin and counterstained with Hoechst (63× magnification). **(B)** HUVEC cells treated as in A were harvested and processed for Rac1 and RhoA activation assays. The left panel shows the WB analysis of GTP-bound Rac1, precipitated by pull-down assay, compared with the total Rac1 (1/20 of input). Histograms represent the densitometry of the GTP-bound Rac1 signals normalized on input. Histograms in the right panel show the measurement of RhoA activation assessed by RhoA G-LISA assay expressed as fold induction of luminescence emissions in treated samples versus negative control (no sample). Purified GTP-bound recombinant RhoA was used as positive control. (**C**) HUVEC cells infected with GFP, Rac1(L61) and RhoA(L63) carrying adenoviruses, were treated and processed for the *in vitro* angiogenesis assay. Bright field images show TS formation (20× magnification), whereas IF images show GFP or anti-Flag staining, merged with Hoechst in the adenovirus infected populations (63× magnification). Histograms represent the quantification of TS formation as mean number of branch points per field in untreated (white bars), VEGF-A stimulated (gray bars) or VEGF-A/RHPS4 treated (black bars) samples. All the experiments were repeated at least three times. Bars indicate means ± SD. $*P < 0.1$; $**P < 0.01$.

targets in oncology, as their stabilization induces transcriptional repression of cancer-related genes. In this context, a recent paper has provided substantive evidence for the formation of G4 structures in the genome of mammalian cells, corroborating the application of stabilizing ligands in a cellular context to target G4 and interfere with gene expression and function (24,25).

Here, by using CD, a valid tool to determine presence and folding of G4 in solution (34–36), we describe, for the first time, the presence of a G4 in the gene promoter of human *vegfr-2,* the main VEGF-A receptor expressed on the surface of EC regulating tumor angiogenesis. Using the same technique, the folding patterns of several G4 promoters have been proposed, including those of molecules involved in angiogenic process such as VEGF (45–47), HIF1α (48,49), platelet-derived growth factor α polypeptide (50,51) and PDGF receptor β polypeptide (52,53). However, there are several novel aspects in our study, which include not only the discovery of a new G4-containg gene but also the functional relevance of this finding through intervention with small molecules, both in cell cultures and in animal model. Specifically, we found that a number of chemically unrelated G4 ligands (26,39,41,42) are able to bind to and stabilize the G4 structure identified within the promoter of *vegfr-2,* providing an explanation for their inhibitory effect on VEGFR-2 expression and on EC proliferation, migration, differentiation and *in vivo* angiogenesis. The effects of G4 ligands

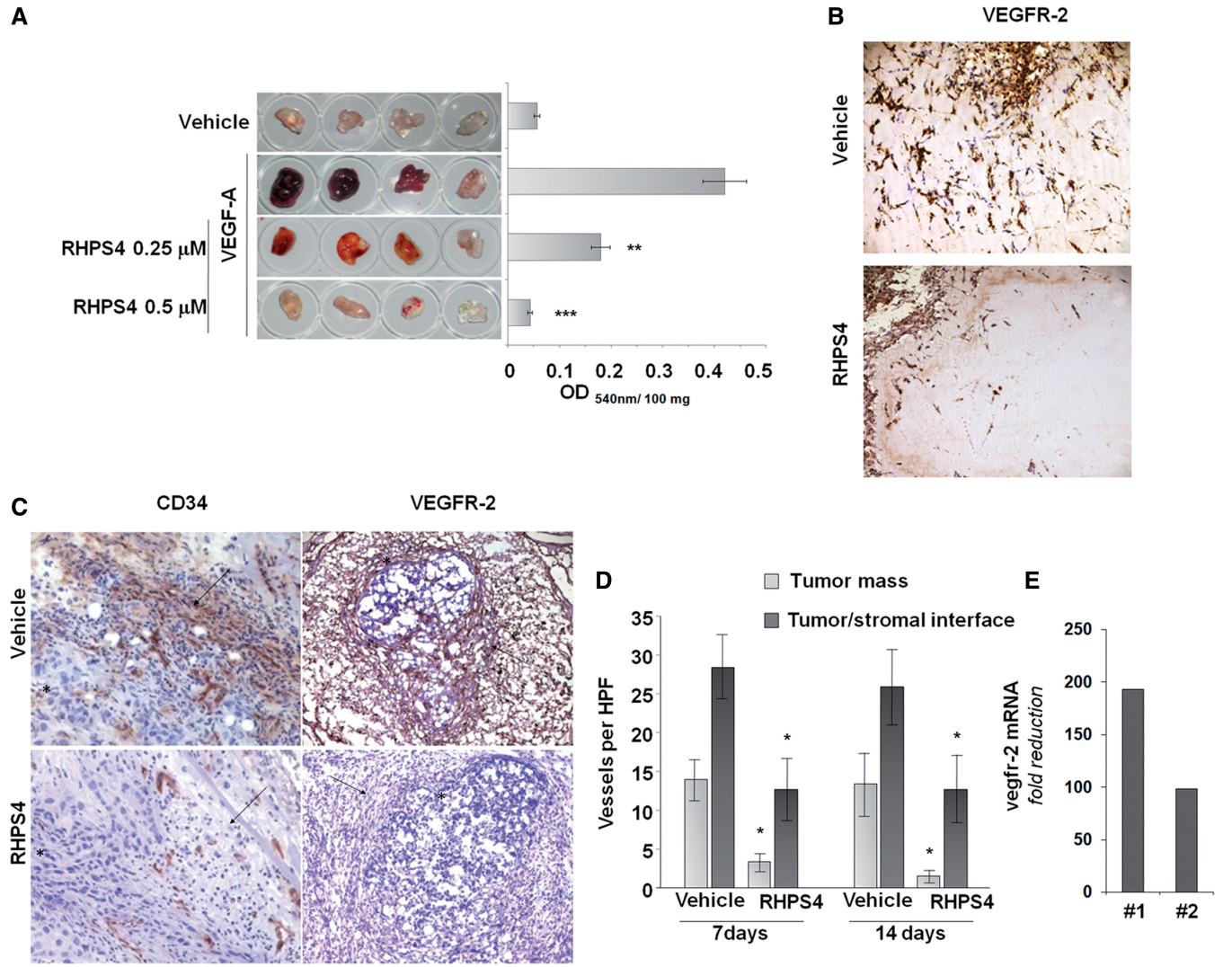

Figure 5. G4 stabilization impairs *in vivo* angiogenesis. (**A**) Matrigel, premixed with VEGF-A and RHPS4 as indicated, was injected subcutaneously into C57 BL/6 mice for the *in vivo* angiogenesis assay. Pictures show Matrigel plugs removed 4 days post injection. Histograms represent the hemoglobin content measured in the relative samples expressed as absorbance (OD 540 nm) per Matrigel mgs. (**B**) Anti-VEGFR-2 immunoperoxidase staining of Matrigel sections in vehicle and RHPS4 containing plugs (100× magnification). (**C**) Tumor sections obtained from RHPS4 treated or untreated tumor xenografted in mice were immunostained with anti-CD34 and anti-VEGFR-2 antibodies. Representative images of tumor mass (asterisk) and peritumoral areas (arrows) are shown (left panels: 200×; right panels: 100× magnification). (**D**) Quantitative analysis of vessel number per HPF in the tumor sections (400× magnification) at the indicated times after cell injection. (**E**) Quantitative analysis of *vegfr-2* mRNA extracted from whole tumor mass, data are reported as vehicle/RHPS4 ratio after b-actin normalization in two different tumors. Histograms in A and D show the mean values of three independent experiments, whereas images in B and C show one representative of three independent experiments with similar results. Bars indicate means ± SD. $*P < 0.1$; $**P < 0.01$; $***P < 0.001$.

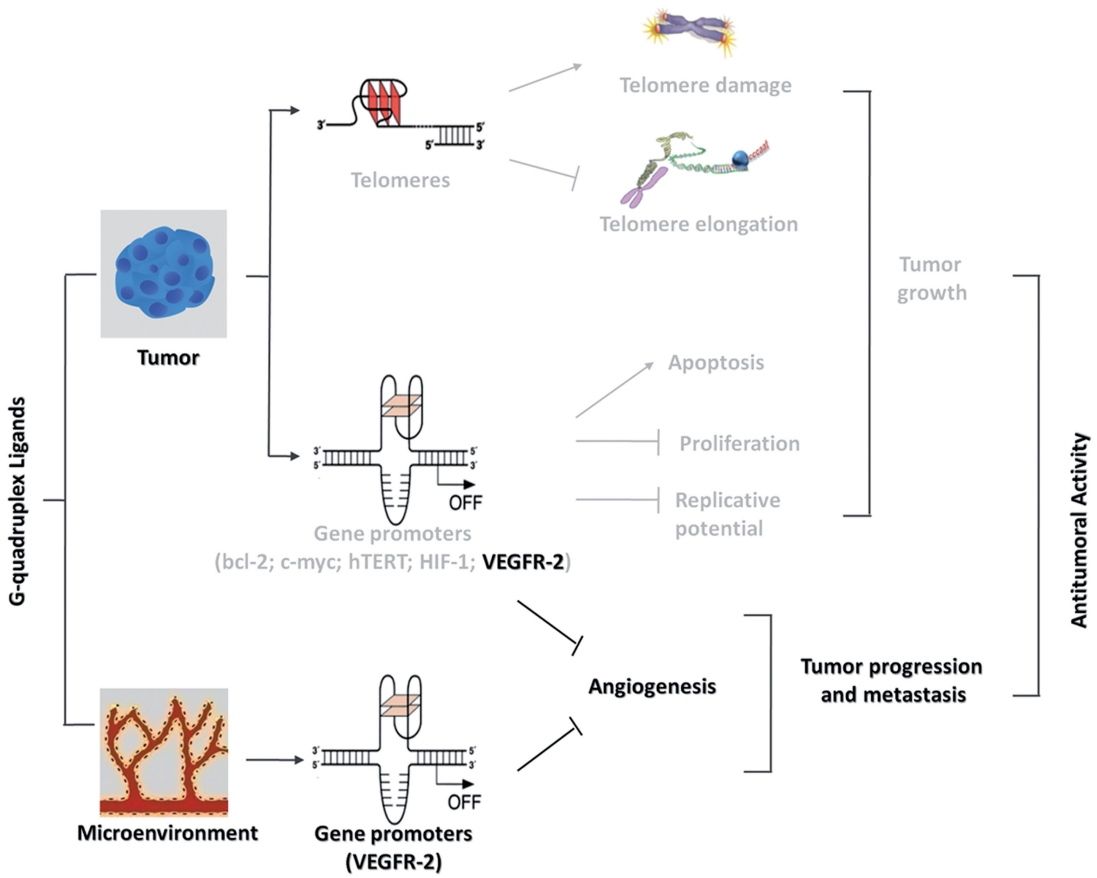

Figure 6. Two-hit antitumor activity of G4 stabilizers. Schematic representation of G4 ligand targets and activity. G4 ligands represent a novel two-hit therapeutic antitumoral strategy, acting on both cancer cells and microenvironment, aimed at blocking tumor growth and progression. From a broader view, G4 ligands can be considered an example of multimodal drugs, combining different therapeutic protagonists in one single component, thus simplifying treatment modality.

have been observed in human- and mouse-derived EC consistently with the presence of the G4 structure in both cell types (54) [as determined by the G4 prediction software QGRS (33)]. Our data show that G4 ligands can exert their antiangiogenic property by directly inhibiting a cell function that is uncoupled from viability, apoptosis, senescence and damage response. Moreover, a strong correlation among the degree of *vegfr-2* promoter stabilization, protein inhibition and impairment of EC functions has been found with the different chemically unrelated G4 ligands, strongly indicating that the biological effects of G4 ligands on EC are linked to their ability to bind to the G4 structure within the *vegfr-2* promoter. A single mutation in the G4 forming sequence of the *vegfr-2* promoter is sufficient to perturb quadruplex formation and to revert the effect of a G4 ligand on *vegfr-2* promoter activity. Moreover, although some other G4 targets were found to be inhibited, the complete rescue of EC function, achieved by the transfection of a *vegfr-2* complementary DNA under the control of a viral promoter, clearly shows that *vegfr-2* is the main target of the G4 ligands regarding angiogenesis.

However, even if we cannot completely exclude that other G4-containing genes can contribute, directly or indirectly, to the inhibition of VEGFR-2, our experiments clearly demonstrate that G4 ligands act on VEGF axis. In particular, G4 ligands specifically inhibit VEGF-A mediated EC functions and angiogenesis as well as VEGF-A mediated activation of RhoA and Rac1, two Rho GTP binding proteins downstream to VEGF/VEGFR-2 signaling. In addition, the effects of small molecules ligands observed on EC recapitulate those observed by using a specific interference RNA against *vegfr-2*. Importantly, the antiangiogenic effect has been also observed *in vivo*. The addition of the G4 ligands to Matrigel plugs strongly inhibited VEGF-A stimulated vessel formation *in vivo,* definitively concluding that our small molecules act on EC.

Consistently with these results, the antiangiogenic effect of RHPS4 has been also observed in tumor tissue by means of CD34 and VEGFR-2 staining. However, in this complex experimental system, we cannot completely exclude that the G4 ligands affect the expression of other angiogenic molecules. In particular, they may directly [acting on other G4-containing endothelial receptors (23)], or indirectly [through inhibition of transcription factors as HIF1α (48,49)], reduce the expression of growth factors and cytokines able to stimulate new blood vessels growth. In conclusion, we describe, for the first time, the antiangiogenic effect of G4 ligands through inhibition of VEGFR-2 and suggest that G4 ligands antiangiogenic properties may significantly contribute to

the antitumoral and antimetastatic activity observed with this class of compounds in preclinical models (26,32).

The data reported in this article provide proof of principle for the potential therapeutic use of targeting G4 structures as novel anticancer strategy. They also highlight a novel two-hit therapeutic strategy, acting on both cancer cells and microenvironment, aimed at blocking tumor growth and progression (Figure 6). Finally, on the basis of the several G4-containing therapeutic targets present in the tumor (Figure 6), from a drug-development perspective, G4 ligands can be an exhaustive example of multimodal class of antineoplastic drug, combing different therapeutic protagonists in one single component, thus simplifying treatment modality, implementing as well selectivity in targeting cancer cells.

SUPPLEMENTARY DATA

Supplementary Data are available at NAR Online, including [55].

ACKNOWLEDGEMENTS

The authors thank Dr Stefano Alemà of the Institute of Cell Biology and Neurobiology CNR (Monterotondo, Rome) and Prof Stefano Cacchione and Dr Alessandra Galati of University 'La Sapienza' of Rome for their kind help with Rho and Rac GTPases activity assays and for DMS footprinting assay, respectively.

FUNDING

Italian Association for Cancer Research [11567 and #9979 to A.B.]; S.I. is recipient of a fellowship from the Italian Foundation for Cancer Research (F.I.R.C.); and A.R. is recipient of a fellowship from the Veronesi Foundation. Funding for open access charge: Italian Association for Cancer Research [11567 to A.B.].

Conflict of interest statement. None declared.

REFERENCES

1. Folkman,J. (1995) Angiogenesis in cancer, vascular, rheumatoid and other disease. *Nat. Med.*, **1**, 27–31.
2. Liotta,L.A., Kleinerman,J. and Saidel,G.M. (1974) Quantitative relationships of intravascular tumor cells, tumor vessels, and pulmonary metastases following tumor implantation. *Cancer Res.*, **34**, 997–1004.
3. Folkman,J. (1990) What is the evidence that tumors are angiogenesis dependent? *J. Natl Cancer Inst.*, **82**, 4–6.
4. Bergers,G. and Benjamin,L.E. (2003) Tumorigenesis and the angiogenic switch. *Nat. Rev. Cancer*, **3**, 401–410.
5. Martiny-Baron,G. and Marme,D. (1995) VEGF-mediated tumour angiogenesis: a new target for cancer therapy. *Curr. Opin. Biotechnol.*, **6**, 675–680.
6. Folkman,J. (2002) Role of angiogenesis in tumor growth and metastasis. *Semin. Oncol.*, **29**, 15–18.
7. Jain,R.K. (2002) Tumor angiogenesis and accessibility: role of vascular endothelial growth factor. *Semin. Oncol.*, **29**, 3–9.
8. Rifkin,D.B. and Moscatelli,D. (1989) Recent developments in the cell biology of basic fibroblast growth factor. *J. Cell Biol.*, **109**, 1–6.
9. Gleave,M.E., Hsieh,J.T., Wu,H.C., Hong,S.J., Zhau,H.E., Guthrie,P.D. and Chung,L.W. (1993) Epidermal growth factor receptor-mediated autocrine and paracrine stimulation of human transitional cell carcinoma. *Cancer Res.*, **53**, 5300–5307.
10. Nicosia,R.F., Nicosia,S.V. and Smith,M. (1994) Vascular endothelial growth factor, platelet-derived growth factor, and insulin-like growth factor-1 promote rat aortic angiogenesis *in vitro*. *Am. J. Pathol.*, **145**, 1023–1029.
11. Davis,S., Aldrich,T.H., Jones,P.F., Acheson,A., Compton,D.L., Jain,V., Ryan,T.E., Bruno,J., Radziejewski,C., Maisonpierre,P.C. *et al.* (1996) Isolation of angiopoietin-1, a ligand for the TIE2 receptor, by secretion-trap expression cloning. *Cell*, **87**, 1161–1169.
12. Maisonpierre,P.C., Suri,C., Jones,P.F., Bartunkova,S., Wiegand,S.J., Radziejewski,C., Compton,D., McClain,J., Aldrich,T.H., Papadopoulos,N. *et al.* (1997) Angiopoietin-2, a natural antagonist for Tie2 that disrupts *in vivo* angiogenesis. *Science*, **277**, 55–60.
13. Inoue,M., Hager,J.H., Ferrara,N., Gerber,H.P. and Hanahan,D. (2002) VEGF-A has a critical, nonredundant role in angiogenic switching and pancreatic beta cell carcinogenesis. *Cancer Cell*, **1**, 193–202.
14. Mustonen,T. and Alitalo,K. (1995) Endothelial receptor tyrosine kinases involved in angiogenesis. *J. Cell Biol.*, **129**, 895–898.
15. Ferrara,N., Gerber,H.P. and LeCouter,J. (2003) The biology of VEGF and its receptors. *Nat. Med.*, **9**, 669–676.
16. Shibuya,M. and Claesson-Welsh,L. (2006) Signal transduction by VEGF receptors in regulation of angiogenesis and lymphangiogenesis. *Exp. Cell Res.*, **312**, 549–560.
17. Olsson,A.K., Dimberg,A., Kreuger,J. and Claesson-Welsh,L. (2006) VEGF receptor signalling - in control of vascular function. *Nat. Rev. Mol. Cell Biol.*, **7**, 359–371.
18. Heasman,S.J. and Ridley,A.J. (2008) Mammalian Rho GTPases: new insights into their functions from *in vivo* studies. *Nat. Rev. Mol. Cell Biol.*, **9**, 690–701.
19. Sitohy,B., Nagy,J.A. and Dvorak,H.F. (2012) Anti-VEGF/VEGFR therapy for cancer: reassessing the target. *Cancer Res.*, **72**, 1909–1914.
20. Han,H. and Hurley,L.H. (2000) G-quadruplex DNA: a potential target for anti-cancer drug design. *Trends Pharmacol. Sci.*, **21**, 136–142.
21. Kelland,L. (2007) Targeting the limitless replicative potential of cancer: the telomerase/telomere pathway. *Clin. Cancer Res.*, **13**, 4960–4963.
22. Neidle,S. (2010) Human telomeric G-quadruplex: the current status of telomeric G-quadruplexes as therapeutic targets in human cancer. *FEBS J.*, **277**, 1118–1125.
23. Balasubramanian,S., Hurley,L.H. and Neidle,S. (2011) Targeting G-quadruplexes in gene promoters: a novel anticancer strategy? *Nat. Rev. Drug. Discov.*, **10**, 261–275.
24. Biffi,G., Tannahill,D., McCafferty,J. and Balasubramanian,S. (2013) Quantitative visualization of DNA G-quadruplex structures in human cells. *Nat. Chem.*, **5**, 182–186.
25. Lam,E.Y., Beraldi,D., Tannahill,D. and Balasubramanian,S. (2013) G-quadruplex structures are stable and detectable in human genomic DNA. *Nat. Commun.*, **4**, 1796.
26. Salvati,E., Leonetti,C., Rizzo,A., Scarsella,M., Mottolese,M., Galati,R., Sperduti,I., Stevens,M.F., D'Incalci,M., Blasco,M. *et al.* (2007) Telomere damage induced by the G-quadruplex ligand RHPS4 has an antitumor effect. *J. Clin. Invest.*, **117**, 3236–3247.
27. Mammoto,A., Connor,K.M., Mammoto,T., Yung,C.W., Huh,D., Aderman,C.M., Mostoslavsky,G., Smith,L.E. and Ingber,D.E. (2009) A mechanosensitive transcriptional mechanism that controls angiogenesis. *Nature*, **457**, 1103–1108.
28. Siddiqui-Jain,A., Grand,C.L., Bearss,D.J. and Hurley,L.H. (2002) Direct evidence for a G-quadruplex in a promoter region and its targeting with a small molecule to repress c-MYC transcription. *Proc. Natl Acad. Sci. USA*, **99**, 11593–11598.
29. Biroccio,A., Benassi,B., Filomeni,G., Amodei,S., Marchini,S., Chiorino,G., Rotilio,G., Zupi,G. and Ciriolo,M.R. (2002) Glutathione influences c-Myc-induced apoptosis in M14 human melanoma cells. *J. Biol. Chem.*, **277**, 43763–43770.

30. Zhang,J., Lu,A., Beech,D., Jiang,B. and Lu,Y. (2007) Suppression of breast cancer metastasis through the inhibition of VEGF-mediated tumor angiogenesis. *Cancer Ther.*, **5**, 273–286.
31. Sander,E.E., ten Klooster,J.P., van Delft,S., van der Kammen,R.A. and Collard,J.G. (1999) Rac downregulates Rho activity: reciprocal balance between both GTPases determines cellular morphology and migratory behavior. *J. Cell Biol.*, **147**, 1009–1022.
32. Leonetti,C., Scarsella,M., Riggio,G., Rizzo,A., Salvati,E., D'Incalci,M., Staszewsky,L., Frapolli,R., Stevens,M.F., Stoppacciaro,A. *et al.* (2008) G-quadruplex ligand RHPS4 potentiates the antitumor activity of camptothecins in preclinical models of solid tumors. *Clin. Cancer Res.*, **14**, 7284–7291.
33. Kikin,O., D'Antonio,L. and Bagga,P.S. (2006) QGRS Mapper: a web-based server for predicting G-quadruplexes in nucleotide sequences. *Nucleic Acids Res.*, **34**, W676–W682.
34. Masiero,S., Trotta,R., Pieraccini,S., De Tito,S., Perone,R., Randazzo,A. and Spada,G.P. (2010) A non-empirical chromophoric interpretation of CD spectra of DNA G-quadruplex structures. *Org. Biomol. Chem.*, **8**, 2683–2692.
35. Karsisiotis,A.I., Hessari,N.M., Novellino,E., Spada,G.P., Randazzo,A. and Webba da Silva,M. (2011) Topological characterization of nucleic acid G-quadruplexes by UV absorption and circular dichroism. *Angew. Chem. Int. Ed. Engl.*, **50**, 10645–10648.
36. Randazzo,A., Spada,G.P. and da Silva,M.W. (2013) Circular dichroism of quadruplex structures. *Top. Curr. Chem.*, **330**, 67–86.
37. Pagano,B., Cosconati,S., Gabelica,V., Petraccone,L., De Tito,S., Marinelli,L., La Pietra,V., di Leva,F.S., Lauri,I., Trotta,R. *et al.* (2012) State-of-the-art methodologies for the discovery and characterization of DNA G-quadruplex binders. *Curr. Pharm. Des.*, **18**, 1880–1899.
38. Leonetti,C., Amodei,S., D'Angelo,C., Rizzo,A., Benassi,B., Antonelli,A., Elli,R., Stevens,M.F., D'Incalci,M., Zupi,G. *et al.* (2004) Biological activity of the G-quadruplex ligand RHPS4 (3,11-difluoro-6,8,13-trimethyl-8H-quino[4,3,2-kl]acridinium methosulfate) is associated with telomere capping alteration. *Mol. Pharmacol.*, **66**, 1138–1146.
39. Gowan,S.M., Heald,R., Stevens,M.F. and Kelland,L.R. (2001) Potent inhibition of telomerase by small-molecule pentacyclic acridines capable of interacting with G-quadruplexes. *Mol. Pharmacol.*, **60**, 981–988.
40. Lamalice,L., Le Boeuf,F. and Huot,J. (2007) Endothelial cell migration during angiogenesis. *Circ. Res.*, **100**, 782–794.
41. Casagrande,V., Salvati,E., Alvino,A., Bianco,A., Ciammaichella,A., D'Angelo,C., Ginnari-Satriani,L., Serrilli,A.M., Iachettini,S., Leonetti,C. *et al.* (2011) N-cyclic bay-substituted perylene G-quadruplex ligands have selective antiproliferative effects on cancer cells and induce telomere damage. *J. Med. Chem.*, **54**, 1140–1156.
42. Franceschin,M., Rizzo,A., Casagrande,V., Salvati,E., Alvino,A., Altieri,A., Ciammaichella,A., Iachettini,S., Leonetti,C., Ortaggi,G. *et al.* (2012) Aromatic core extension in the series of N-cyclic bay-substituted perylene G-quadruplex ligands: increased telomere damage, antitumor activity, and strong selectivity for neoplastic over healthy cells. *ChemMedChem*, **7**, 2144–2154.
43. Beckers,C.M., van Hinsbergh,V.W. and van Nieuw Amerongen,G.P. (2010) Driving Rho GTPase activity in endothelial cells regulates barrier integrity. *Thromb Haemost*, **103**, 40–55.
44. Connolly,J.O., Simpson,N., Hewlett,L. and Hall,A. (2002) Rac regulates endothelial morphogenesis and capillary assembly. *Mol. Biol. Cell*, **13**, 2474–2485.
45. Sun,D., Guo,K., Rusche,J.J. and Hurley,L.H. (2005) Facilitation of a structural transition in the polypurine/polypyrimidine tract within the proximal promoter region of the human VEGF gene by the presence of potassium and G-quadruplex-interactive agents. *Nucleic Acids Res.*, **33**, 6070–6080.
46. Sun,D., Guo,K. and Shin,Y.J. (2011) Evidence of the formation of G-quadruplex structures in the promoter region of the human vascular endothelial growth factor gene. *Nucleic Acids Res.*, **39**, 1256–1265.
47. Taka,T., Joonlasak,K., Huang,L., Randall Lee,T., Chang,S.W. and Tuntiwechapikul,W. (2012) Down-regulation of the human VEGF gene expression by perylene monoimide derivatives. *Bioorg. Med. Chem. Lett.*, **22**, 518–522.
48. De Armond,R., Wood,S., Sun,D., Hurley,L.H. and Ebbinghaus,S.W. (2005) Evidence for the presence of a guanine quadruplex forming region within a polypurine tract of the hypoxia inducible factor 1alpha promoter. *Biochemistry*, **44**, 16341–16350.
49. Lombardo,C.M., Welsh,S.J., Strauss,S.J., Dale,A.G., Todd,A.K., Nanjunda,R., Wilson,W.D. and Neidle,S. (2012) A novel series of G-quadruplex ligands with selectivity for HIF-expressing osteosarcoma and renal cancer cell lines. *Bioorg. Med. Chem. Lett.*, **22**, 5984–5988.
50. Qin,Y., Rezler,E.M., Gokhale,V., Sun,D. and Hurley,L.H. (2007) Characterization of the G-quadruplexes in the duplex nuclease hypersensitive element of the PDGF-A promoter and modulation of PDGF-A promoter activity by TMPyP4. *Nucleic Acids Res.*, **35**, 7698–7713.
51. Viglasky,V. (2009) Platination of telomeric sequences and nuclease hypersensitive elements of human c-myc and PDGF-A promoters and their ability to form G-quadruplexes. *FEBS J.*, **276**, 401–409.
52. Qin,Y., Fortin,J.S., Tye,D., Gleason-Guzman,M., Brooks,T.A. and Hurley,L.H. (2010) Molecular cloning of the human platelet-derived growth factor receptor beta (PDGFR-beta) promoter and drug targeting of the G-quadruplex-forming region to repress PDGFR-beta expression. *Biochemistry*, **49**, 4208–4219.
53. Chen,Y., Agrawal,P., Brown,R.V., Hatzakis,E., Hurley,L. and Yang,D. (2012) The major G-quadruplex formed in the human platelet-derived growth factor receptor beta promoter adopts a novel broken-strand structure in K+ solution. *J. Am. Chem. Soc.*, **134**, 13220–13223.
54. Patterson,C., Perrella,M.A., Hsieh,C.M., Yoshizumi,M., Lee,M.E. and Haber,E. (1995) Cloning and functional analysis of the promoter for KDR/flk-1, a receptor for vascular endothelial growth factor. *J. Biol. Chem.*, **270**, 23111–23118.
55. Sun,D. and Hurley,L.H. (2010) Biochemical techniques for the characterization of G-quadruplex structures: EMSA, DMS footprinting, and DNA polymerase stop assay. *Methods Mol. Biol.*, **608**, 65–79.